

Effects of shot speed and biscuit thickness on externally solidified crystals of high-pressure die cast AM60B magnesium alloy

WANG Bai-shu^{1,2}, XIONG Shou-mei¹

1. State Key Laboratory of Automotive Safety and Energy,

Department of Mechanical Engineering, Tsinghua University, Beijing 100084, China;

2. Key Laboratory of Advanced Structural Materials of Ministry of Education,

Department of Materials Science and Engineering, Changchun University of Technology, Changchun 130012, China

Received 25 September 2010; accepted 22 December 2010

Abstract: Standard mechanical test bars with a diameter of 6.4 mm and a gauge length of 50 mm were processed, and the microstructures of die cast AM60B alloy under different die casting process parameters were observed. The influences of the slow shot speed, the fast shot speed and the biscuit thickness on the externally solidified crystals (ESCs) were investigated. With the increase of the biscuit thickness, the number of the ESCs in the cast samples decreases. Under a low slow shot speed, large ESCs are found in the cast structure and a high fast shot speed results in more spherical ESCs. The relationships between ESCs and process parameters were also discussed.

Key words: AM60B magnesium alloy; die casting; microstructure; externally solidified crystals

1 Introduction

In a cold-chamber die casting process, the alloy melt in a furnace is transferred to the shot sleeve after die clamping, followed by a slow shot phase, a fast shot phase and a pressure intensification phase pour[1], and the die cast parts will be extracted after the die is opened. During this process, the cooling occurs in the ladle, shot chamber and runner and die cavity. There is a high heat-transfer coefficient among the liquid metal and the shot sleeve and the plunger tip, etc, before the melt is injected into die cavity through the gate[2]. Besides the sludge, oxide inclusions and oxide films as externally solidified phases in high-pressure die casting (HPDC) alloys, typical die casting produces 5%–15% externally solidified materials in the shot sleeve before the liquid (plus solid) is forced into the die cavity[3]. The co-existence of coarse and fine primary grains is often found in HPDC products. The relatively coarse grains begin their solidification in the shot chamber and are known as the externally solidified crystals (ESCs). The defect band characteristics and the ESCs have been

studied in HPDC magnesium alloys[4–5]. However, the microstructure characterization and analysis based on the ESCs have been performed very little for the HPDC magnesium alloy. YU et al[6] referred to the relative coarse primary phase. In this study, some detailed microstructure characteristics of the ESCs of HPDC AM60 alloy were presented.

2 Experimental

Standard mechanical test bars with a diameter of 6.4 mm and a gauge length of 50 mm were processed with HPDC process. The diameter of the shot chamber was 70 mm and the length was 342 mm. The calculated fill ratio was 17.1% when the thickness of the biscuit was 20 mm; the area ratio of the shot plunger and the gate was 46.2. The HPDC parameters, including a casting temperature of 680 °C, a die temperature of 150 °C, different slow shot speeds from 0.1 to 0.8 m/s, different fast shot speeds from 1.25 to 2.25 m/s and different thicknesses of biscuits, were taken into account.

All of the metallographic specimens were etched with the diluted acetic acid solution, which comprised 50

mL distilled water, 150 mL anhydrous ethyl alcohol and 1 mL glacial acetic acid. The microstructures were observed with an optical microscope.

3 Results and discussion

3.1 Effect of slow shot velocity on ESCs

Figures 1(a)–(d) show the microstructures of the central cross section of the HPDC bars with a biscuit thickness of about 20 mm, at a fast shot speed of 1.75 m/s and at different slow shot speeds of 0.1, 0.3, 0.5 and 0.7 m/s, respectively.

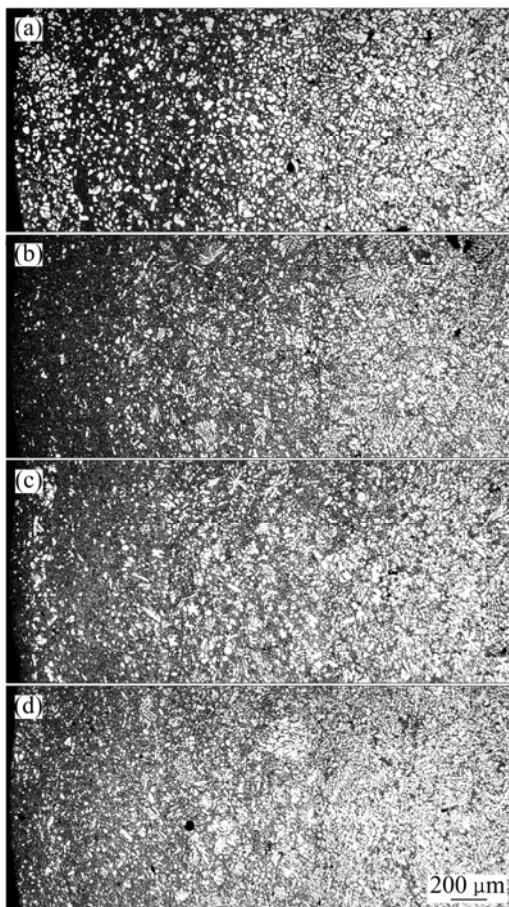


Fig.1 OM micrographs of central cross section of HPDC bars with biscuit thickness of about 20 mm, at fast shot speed of 1.75 m/s and at different slow shot speeds: (a) 0.1 m/s; (b) 0.3 m/s; (c) 0.5 m/s; (d) 0.7 m/s

According to the experimental record, the slow shot distance is 273 mm and the fast shot distance is 48 mm. The calculated slow shot time is 2.73, 0.91, 0.55 and 0.39 s, respectively; and the fast shot time is 0.027 s. Therefore, the corresponding total residence time of metal melt in the shot sleeve is about 2.76, 0.94, 0.58 and 0.42 s regardless of the shot delay. Such residence time is meaningful for the superheat loss of the melt and consequently for real crystal growth, as shown in Fig.1. The ESCs in the microstructure with the residence time

of 2.76 s are the coarsest and those with the residence time of 0.39 s are the finest; while the ESCs with the residence time of 0.58 s are mildly coarser than those with the residence time of 0.94 s. The crystal growth will proceed with time in the metal melt and at last the size of ESCs is large for a long residence time in the shot sleeve. The size of ESCs with the residence time of 0.58 s is not suitable for such an ordination. The free crystals are initiated from different sources. Some of them nucleate on the interior surface of the shot chamber, at the air-liquid interface, or in the region where the melt temperature falls below the liquidus, and then grows up; some others are from the solid shell.

When the liquid metal is poured into the shot sleeve, the cooling and the resultant superheat loss will occur at once. Normally, the shot starts once the pouring finishes and an explicit shot delay does not exist. The shot and the cooling proceed simultaneously. Solidification of the liquid metal occurs from the interface with the interior surface of the shot sleeve and the plunger tip, and a temperature gradient forms and a portion of liquid metal which is away from the shell may be above the liquidus till the shot finishes. The plunger will squeeze the solid shell and peel it off from the shot sleeve, and during this movement, the resultant deformation and fracture make the solid shell break into some pieces. Besides, these fragmented pieces that comprise more than one primary crystal and some fragmented dendrites are broken away from the solid-liquid interface and some dendrites leave the solid shell, and they will drift away from the solid-liquid interface and become free. As a result of the slow plunger movement, the fluid movement will involve some of the pieces and the free crystals into the liquid metal, and then on-going mixing proceeds. In this process, some crystals will remelt and some are going to grow up because of poor uniformity in temperature and solute concentration.

As the slow shot speed increases, the deformation rate of the solid shell becomes larger and more crystals enter into the melt. Meanwhile, the uniformity of the melt also becomes better and more crystals will remelt and the resultant shrink proceeds faster. Therefore, the effect of the shot process is complex for the morphology of the ESCs. Of course, the regulation accuracy of the shot delay can affect the total residence time, more precisely, the growing time of the crystals. Similar to the size of the ESCs, there is a similar ordination for the density and number of ESCs, as shown in Fig. 1.

3.2 Effect of fast shot velocity on ESCs

Figure 2 shows the microstructures of the central cross section of the HPDC bars with a biscuit thickness of about 20 mm, at a slow shot speed of 0.4 m/s and at

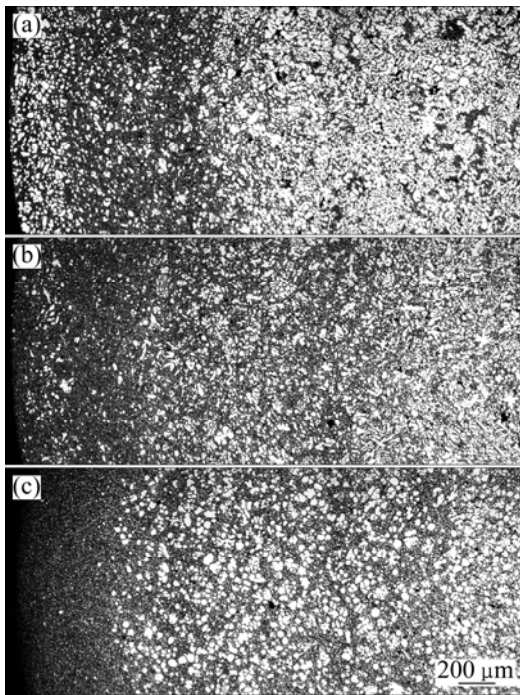


Fig.2 OM micrographs of central cross section of HPDC bars with biscuit thickness of about 20 mm, at slow shot speed of 0.4 m/s and at different fast shot speeds: (a) 1.25 m/s; (b) 1.75 m/s; (c) 2.25 m/s

different fast shot speeds of 1.25, 1.75, 2.25 m/s, respectively.

Unlike the slow shot speed, the fast shot does not affect the residence time of the melt in the shot sleeve significantly. According to the results in Fig.2, the size of ESCs with a fast shot speed of 1.75 m/s is the smallest among them and the development degree of the dendrite of the ESCs is the highest too. In this case, the effect of the plunger movement on the melt should be paid more attention to.

The melt mixture is injected into the die cavity while the fast shot starts. A highly intense mixing occurs while the melt passes the gate. The degree of the intensity depends on the speed of the fast shot phase. A relatively low speed of 1.25 m/s in the fast shot phase leads to a poor mixture, then more crystals can grow up. On the contrary, a relatively high speed of 2.25 m/s leads to a good mixture, then less crystals grow up and more dendrites are degraded because of the intensified flow shear. At the same time, new nucleation and the growth of those nucleus will be suppressed, and as a result, the crystals in the melt mixture will grow up with spheroidization as the melt temperature drops in the die cavity. At last, the existed pre-solidified crystals will grow into such a stability[7], i.e., from a very high speed to a very low speed. New nucleation and growth-up will continue because of thermodynamics and the relatively fine primary crystals are also obtained, and then the final

eutectic solidification for AM60 alloy at last. Therefore, a semi-solid rheological microstructure is obtained with coarse sphere grains at the fast shot speeds of 2.25 m/s.

In a word, there is difference in microstructure because the fast shot speed affects the mixing level, the intensity of flow shear and the grain growth, as shown in Fig.2.

3.3 Effect of biscuit thickness on ESCs

Figure 3 shows the microstructures of the central cross section of the HPDC bars at a slow shot speed of 0.4 m/s, at a fast shot speed of 1.75 m/s and with different biscuit thicknesses of 13, 23, 32, 42, 52, 65 mm, respectively.

According to the practical measurement, the mass of a whole HPDC product with a biscuit thickness of 20 mm is 390 g. The mass of the poured liquid metal increases by 6.9 g with an increase of the biscuit thickness per millimeter. When the biscuit thickness increases, more liquid metal is poured into the shot sleeve, and the melt can retain higher temperature while it enters into the die cavity under the same shot process. Because of similar residence time, the size and the density of the free crystals with different poured liquid volumes will be affected mainly by the resultant retained temperature, and as a result, the size and the density of ESCs in the parts decrease with the increase of the biscuit thickness, as shown in Figs.3(b)–(f). The exception shown in Fig.3(a) can be understood from the retained low melt temperatures too. A low pouring temperature and a small poured volume will lead to a large content of solid (shell) in the melt, and more free crystals survive in higher solute concentration of the remnant liquid so that the free crystals will grow slowly in the higher solution concentration of the melt and in a short time because of low temperature and little liquid, smaller ESCs are obtained. The low density in Fig.3(a) can be understood that a high volume of solid blocks the mixed melt to enter the die cavity through the runner and gate; at last, more liquid permeates into the die cavity through the crowded solid pieces under the condition of the relatively low shot sleeve filling ratio of 17.1%.

3.4 Inhomogeneous ESC distribution and other microstructure phenomena

Firstly, there is a difference in the ESC distribution between the skin and the central region. The density of ESCs near surface is lower than that of the central region; there are more sphere ESCs near the surface and more dendrites in the center with respect to morphology, as shown in Figs.1–3. From surface to center, the density of ESCs increases[8] and an example is presented in Fig.2(c) with an ESC-free skin of about 400 μm in thickness. The

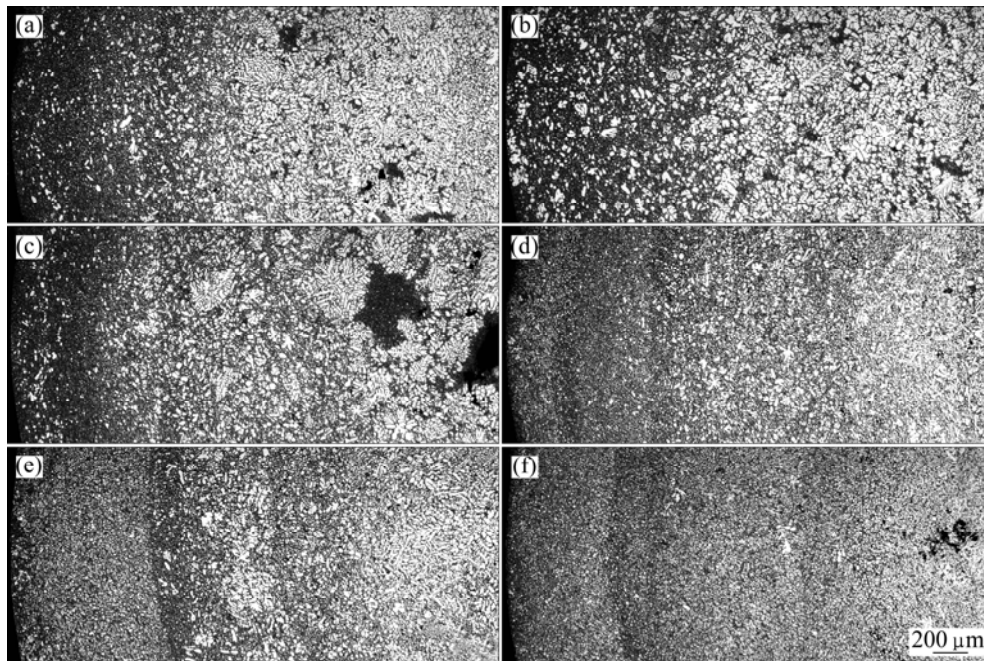


Fig.3 OM micrographs of central cross sections of HPDC bars at slow shot speed of 0.4 m/s, at fast shot speed of 1.75 m/s and with different biscuit thicknesses: (a) 13 mm; (b) 23 mm; (c) 32 mm; (d) 42 mm; (e) 52 mm; (f) 65 mm

ESC distribution can be explained that the flow shear induces the migration of ESCs toward the center in the solid and liquid mixture[9]. In some samples, the density of ESCs is larger in the most external layer than that in the sub-surface region, as shown in Fig.1(c), Fig.2 and Fig.3(c). This can be explained not only by the flow shear but also the rapid solidification in the die cavity. The rapid cooling directly can freeze the coarse crystals so as to catch them in the solid skin, or the high viscosity of melt near interface can stick those coarse crystals to prevent the migrate toward the central region.

Secondly, besides the skin, one or multiple dark loops can be observed on some etched samples in Figs.1–3, and the bands are parallel to the surface contour of bars[5].

Thirdly, there is a difference in the ESC distribution in the skin between near the gate area and the overflow area of same test bar, as shown in Figs.4(a) and (b), which relates to joint impact of solidification and flow shear. Not all of the HPDC bars present such a feature.

Fourthly, in the central region of a bar, a developed dendrite, an ESC-free skin micro-area and a big pore are shown in Fig.3(c). The developed dendrite and the ESC-free micro-area are furthermore observed in the magnification micrographs in Figs.5(a) and (b), respectively. The third branch can be distinguished in a dendrite with above 300 μm of size, and some very fine primary dendrites can be found among the black eutectics in Fig.5(b).

Fifthly, some of the primary phases nucleate and

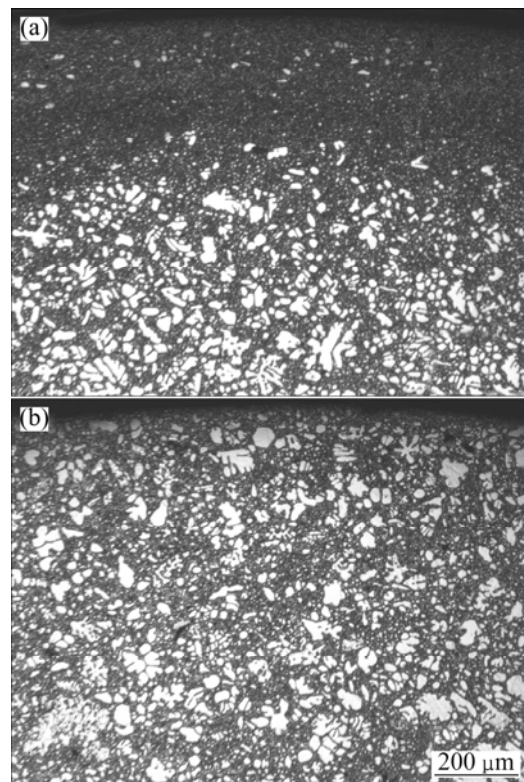


Fig.4 OM micrographs near gate (a) and overflow (b) of selected HPDC bar

grow up in the same place such as the shot chamber or the die cavity, and the growth of some primary phases proceeds in the die cavity on the existed crystals for AM60 alloy. Some fine cells like fingers designated by arrows attach the tip of the secondary dendrite arms of a

coarse dendrite, as shown in Fig.6. The coarse dendrite nucleated and slowly grew up in the shot sleeve, and then a rapid secondary growth proceeded based on the dendrite in the die cavity, and the fine finger-shape cells were obtained during the rapid solidification in the die cavity. This phenomenon is an example of growth instability occurred in a HPDC process[7].

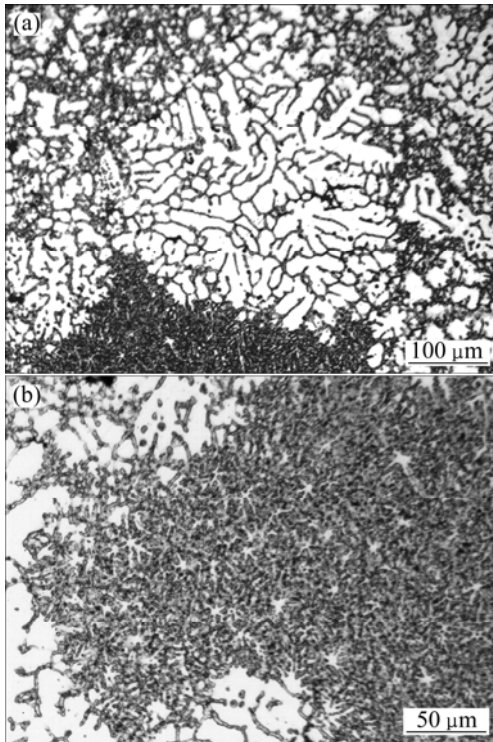


Fig.5 OM micrographs of developed dendrite (a) and black ESCs-free region (b) in HPDC bar

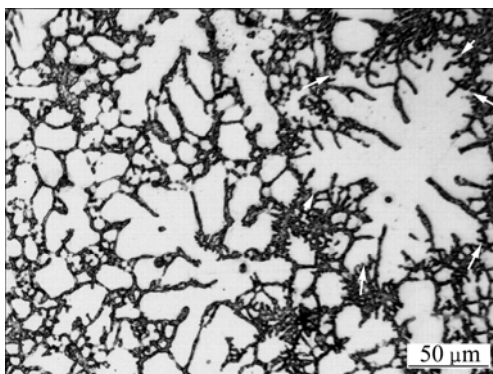


Fig.6 OM micrographs of dendrite with growth instability phenomenon in selected area (The fine cells like fingers pointed by arrows grew on the dendrite tip in the die cavity)

At last, a piece of externally solidified materials can be judged by a crowd of fine cells and the black porosities in Fig. 7. The crack of the porosity in the externally solidified materials was initiated by the squeezing deformation during the plunger movement. Such external solid debris broken from the solid shell

may have an influence on mechanical properties in the relative study and the externally solidified materials with oxide surface are called as cold flake[10].

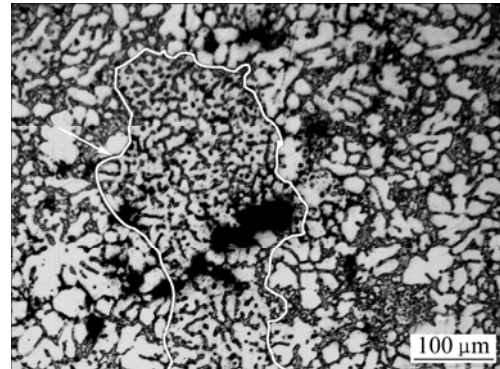


Fig.7 OM micrograph of externally solidified materials in microstructure of a HPDC bar

4 Conclusions

1) With the increase of the biscuit thickness, the density, the size of the ESCs in the cast parts decrease. At a low slow shot speed, large ESCs are found in the cast structure. A high fast shot speed results in more spherical ESCs.

2) The slow shot phase is mainly made up of the residence time of the cast alloy in the shot sleeve, which determines the quantity of the superheat loss of the poured liquid alloy. The fast shot velocity sets the intensity of the flow shear and further affects the distribution and the spheroidization level of ESCs.

3) The inhomogeneous characteristics of ESCs in the HPDC parts are presented. The distribution of ESCs is different in different positions, such as near the surface, in the interior, near the gate and the overflow. Sometimes the banded microstructure, the coarse developed dendrite, the large size of ESC-free area or the large pore appears, and there are some pieces of externally solidified materials in a HPDC part.

References

- [1] LUI Y B, LEE W B, RALPH B. A reclassification of the die-filling stages in pressure die-casting processes [J]. *Journal of Materials Processing Technology*, 1996, 57(3-4): 259-265.
- [2] HELENIUS R, LOHNE O, ARNBERG L, LAUKLI H I. The heat transfer during filling of a high-pressure die-casting shot sleeve [C]//International Conference on Advances in Solidification Processes. Stockholm, Sweden: Materials Science Engineering A-Structural Materials Properties Microstructure and Processing, 2005: 52-55.
- [3] TSUMAGARI N, BREVICK J R, MOBLEY C E. Control of microstructures in aluminum alloy diecastings [C]//2nd Annual Meeting of the American-Foundrymen's-Society. Atlanta GA: AFS Transactions, 1998: 15-20.

- [4] CAO H, WESSÉN M. Characteristics of microstructure and banded defects in die cast AM50 magnesium components [J]. International Journal Cast Metals Research, 2005, 18(6): 377-384.
- [5] GOURLAY C M, LAUKLI H I, DAHLE A K. Defect band characteristics in Mg-Al and Al-Si high-pressure die castings [J]. Metallurgical Materials Transactions A, 2007, 38(8): 1833-1844.
- [6] YU Peng, ZHANG Jing-huai, TANG Ding-xiang, LIU Ke, MENG Jian, ZHOU De-feng. Microstructures and mechanical properties of high-pressure die-cast Mg-4A-0.4Mn-xPr alloys [J]. The Chinese Journal of Nonferrous Metals, 2009, 19(5): 833-840. (in Chinese)
- [7] MARTINEZ R A, KARMA A, FLEMINGS M C. Spheroidal particle stability in semisolid processing [J]. Metallurgical and Materials Transactions A, 2006, 37(9): 2807-2815.
- [8] LAUKLI H I, GOURLAY C M, DAHLE A K. Migration of crystals during the filling of semi-solid castings [J]. Metallurgical Materials and Transaction A, 2005, 36(3A): 805-818.
- [9] GOURLAY C M, DAHLE A K. Dilatant shear bands in solidifying metals [J]. Nature, 2007, 445(7123): 70-73.
- [10] AHAMED A K M A, KATO H. Effect of cold flakes in mechanical properties of aluminum alloy die-casts [C]//Proceedings of 10th Asian Foundry Congress (AFC10). Nagoya, Japan, 2008: 461-466.

压射速度和料饼厚度对压铸AM60B镁合金 压室预结晶的影响

王柏树^{1,2}, 熊守美¹

1. 清华大学 机械工程系 汽车安全与节能国家重点实验室, 北京 100084;
2. 长春工业大学 材料科学与工程学院 先进结构材料省部共建教育部重点实验室, 长春 130012

摘要: 采用不同的慢压射速度、快压射速度和不同的料饼厚度, 压铸直径6.4 mm、标距长度50 mm的标准拉伸试样, 观察压铸试样的显微组织, 分析不同工艺对压室预结晶的影响, 讨论压室预结晶与工艺参数的关系。结果表明: 随着料饼厚度的增加, 组织中的压室预结晶数量减少; 低的慢压射速度可获得较大尺寸的压室预结晶; 高的快压射速度有利于形成球状的压室预结晶。

关键词: AM60B镁合金; 压铸; 组织; 压室预结晶

(Edited by LI Xiang-qun)